

EFFECTS OF EXTERNAL CESIUM AND RUBIDIUM ON OUTWARD POTASSIUM CURRENTS IN SQUID AXONS

JOHN R. CLAY

Section on Neural Membranes, Laboratory of Biophysics, Intramural Research Program, National Institute of Neurological and Communicative Disorders and Stroke, National Institutes of Health at the Marine Biological Laboratory, Woods Hole, Massachusetts 02543

MICHAEL F. SHLESINGER

Institute for Physical Sciences and Technology, University of Maryland, College Park, Maryland 20742 and the La Jolla Institute, La Jolla, California 92038

ABSTRACT We have studied the effects of external cesium and rubidium on potassium conductance of voltage clamped squid axons over a broad range of concentrations of these ions relative to the external potassium concentration. Our primary novel finding concerning cesium is that relatively large concentrations of this ion are able to block a small, but statistically significant fraction of outward potassium current for potentials less than ~ 50 mV positive to reversal potential. This effect is relieved at more positive potentials. We have also found that external rubidium blocks outward current with a qualitatively similar voltage dependence. This effect is more readily apparent than the cesium blockade, occurring even for concentrations less than that of external potassium. Rubidium also has a blocking effect on inward current, which is relieved for potentials more than 20–40 mV negative to reversal, thereby allowing both potassium and rubidium ions to cross the membrane. We have described these results with a single-file diffusion model of ion permeation through potassium channels. The model analysis suggests that both rubidium and cesium ions exert their blocking effects at the innermost site of a two-site channel, and that rubidium competes with potassium ions for entry into the channel more effectively than does cesium under comparable conditions.

INTRODUCTION

The permeability of the potassium channel of nerve axon membrane to potassium ions can be modified by all of the other alkali metal cations (see French and Adelman, 1976 *a*; and Hille and Schwartz, 1978, for reviews). For example, outward potassium ion current is reduced by the addition of either lithium, sodium, cesium, or rubidium to the internal solution bathing the axonal membrane (Chandler and Meves, 1965; Adelman and Senft, 1966; Bezanilla and Armstrong, 1972; French and Wells, 1977). Externally, only cesium and rubidium have clear effects on channel conductance (Pickard et al., 1964; Bezanilla and Armstrong, 1972; Hille, 1973; Adelman and French, 1978). Sodium and lithium ions appear to be unable to enter the potassium channel from the external solution (Bezanilla and Armstrong, 1972; Hille, 1973). The only alkali metal ion that can readily pass through the channel, other than potassium itself, is rubidium (Pickard et al., 1964; Hille, 1973). Cesium, sodium, and lithium act chiefly as blockers of potassium channels. The effects of all of these ions appear to take place virtually instantaneously after a voltage step is made in voltage-clamp conditions. That is, their effects are principally voltage dependent and not time dependent. They act chiefly on outward rather

than inward current when they are placed in the internal solution, whereas they act chiefly on inward current when they are placed in the external solution. For example, internal sodium has little or no effect on inward potassium ion current (French and Wells, 1977). The qualitative similarity of the effects of internal lithium, cesium, and rubidium to the effects of sodium suggests that none of these ions modifies inward current when they are placed internally (Adelman, 1971; Bezanilla and Armstrong, 1972; French et al., 1979). The effects of external rubidium and cesium on outward potassium ion current are less well understood. Pickard et al. (1964) reported no such effect for cesium. French and Adelman (1976 *b*) reported an augmentation of outward current by external cesium, although they later cautioned that this result might have been attributable to a reduction of potassium channel block by Tris buffer in experiments in which Tris was replaced by cesium (Adelman and French, 1978). Voltage-clamp results in the literature suggest that external rubidium reduces outward current (Pickard et al., 1964; Hille, 1973; Swenson and Armstrong, 1981), although the dependence of this effect on voltage and on external rubidium ion concentration has not been previously described.

We have investigated the effects of external cesium, rubidium, potassium, and Tris, principally on outward

current for a broad range of concentrations of these ions, using internally perfused squid axons. The external ionic strength was maintained constant by replacing the external sodium in our control artificial seawater with the test ion. We confirm that solutions containing high concentrations of Tris reduce outward potassium ion current during voltage-clamp depolarization, although they appear to do so by slowing potassium channel activation rather than by blocking the channel itself. We also report a small, but statistically significant reduction of outward current by external cesium when the cesium concentration is significantly greater than the external potassium concentration. This effect occurs for potentials less than ~ 50 mV positive to the reversal potential. The test and the control currents are statistically the same at more positive potentials. Blockade of outward current by external rubidium is more readily apparent. This effect occurs even for rubidium concentrations that are less than the external potassium concentration. The voltage dependence of this effect is similar to that of cesium.

We have modeled our results by assuming that ion permeation occurs via knock-on single-file diffusion of ions through a multisite channel (Hodgkin and Keynes, 1955; Hladky, 1965; Hladky and Harris, 1967; Clay and Shlesinger, 1977). Blockade by cesium or rubidium is assumed to occur at one of the sites within the channel. Rubidium ions are permitted to be knocked from the blocking site to the internal solution by external ions. This feature of the model accounts for the permeability of the channel to rubidium. A primary result of our analysis is an estimate for the parameter which describes the competition of either cesium or rubidium with external potassium for entry into the potassium channel. A preliminary report of some of these results has been given (Clay and Shlesinger, 1982).

METHODS

Experimental Preparation

The experiments described in this paper were carried out on internally perfused squid axons. Squid (*Loligo pealei*) were provided by the Marine Biological Laboratory, Woods Hole, MA. Our methods were generally the same as those of French and Shoukimas (1981). A low impedance axial wire voltage-clamp system was used to control the transmembrane potential V . We compensated for $2\Omega\cdot\text{cm}^2$ of series resistance. Settling time for the current trace in response to a hyperpolarizing voltage pulse was $\leq 20\ \mu\text{s}$. Glass pipettes of 50–80 μm tip diameter filled with 0.5 M KCl in 1–2% agar were used as internal and external voltage-sensing electrodes. A floating platinum wire shunt in the pipettes reduced the high-frequency impedance (Fishman, 1973). The axial wire was fixed concentrically within the perfusion cannula. This arrangement and the internal voltage sensing electrodes were placed inside the axon from opposite directions through holes cut in both ends of the preparation. Perfusion was initiated without the use of enzymes by passing the cannula through the axon one or more times using suction to remove the axoplasm. The temperature of the external solution was maintained at $8 \pm 0.1^\circ\text{C}$ during data acquisition. External solutions flowed over the axon at a rate of $\sim 5\ \text{ml}\cdot\text{min}^{-1}$ (chamber volume $\sim 0.05\ \text{ml}$). In all experiments the sodium conductance was suppressed by the addition of $0.5\ \mu\text{M}$ tetrodotoxin (TTX) to the external solution.

Solutions

The internal perfusate that was used in all of our experiments consisted of 50 mM KF, 200 mM K Glutamate, 25 mM K_2HPO_4 , and 505 mM sucrose. The internal pH was adjusted to 7.2 ± 0.1 at a room temperature of $\sim 20^\circ\text{C}$. The ionic composition of our external artificial seawater (ASW) solutions was 50 mM Mg^{++} , 10 mM Ca^{++} , 561 mM Cl^- , and Na^+ , K^+ , Cs^+ , and Rb^+ as given in Table I. The labels given in the first column of Table I will be used throughout this paper for identification purposes. All solutions except for the 10 mM K 440 mM Tris SW (not listed in Table I) were buffered by 1 mM Tris (Tris-hydroxymethylaminomethane-HCl). The 10 mM K 400 mM Tris SW consisted of 430 mM Tris, 50 mM MgCl_2 , 10 mM CaCl_2 , and 10 mM KCl. The external pH at room temperature was adjusted to 7.0 ± 0.1 .

Experimental Protocol

The principal aim of these experiments was to determine the relative voltage dependence of potassium-channel current for as broad a range as possible of the ratio of either external cesium or rubidium to external potassium concentration. At the same time, we wanted to minimize potassium ion accumulation in the periaxonal space during prepulse activation of conductance with an appropriate level of external K. We found that 100 mM K was a reasonable compromise to these two conflicting constraints. Consequently, the bulk of our measurements were carried out with 100 mM K SW as our control external solution. We used a 20-ms duration prepulse to either $V = -20$ mV (inside negative) or $V = 0$ mV to partially activate potassium channel conductance. Axons were held at either -80 or -100 mV during the time between pulses and during changes in external solutions. Membrane current was measured isochronally 50 μs following initiation of a 5-ms duration test potential step to -140 , -120 , \dots , $+80$ mV with a 5 s rest interval between each measurement of this sequence. A disadvantage of this protocol was that potassium conductance was a function of time during the test pulse. It was activated still further by positive-going pulses and it was deactivated by negative-going test pulses. However, the time constants of channel conductance at 8°C were a few milliseconds or longer for all test potentials. Consequently, the error introduced into our measurements by voltage-dependent channel kinetics was at most 2–3%.

A further potential source of error was that a change of external solution might alter activation kinetics during the prepulse. The evidence against this effect is as follows.

(a) The rising phase of membrane current (~ 5 – 10 ms) following depolarizations that produced outward current both in 100 and 500 mM K SW superposed almost exactly after appropriate scaling. A similar result was obtained with Rb SW compared with the 100 mM K SW control. Moreover, activation kinetics in Cs SW superposed with the control kinetics, following appropriate scaling, throughout the duration of 20 ms depolarizations from holding potential.

TABLE I
COMPOSITION OF EXTERNAL SOLUTIONS

Solution	K^+	Na^+	Cs^+	Rb^+
10 K SW	10	430		
50 K SW	50	390		
100 K SW	100	340		
300 K SW	300	140		
500 K SW*	500			
100 K \times Cs SW	100	340-x	x	
100 K \times Rb SW	100	340-x		x
10 K 340 Cs SW	10	90	340	
0 K 340 Rb SW	0	100		340
0 K 340 Cs SW	0	100	340	

All concentrations are given in millimolar units.

*This solution contained 500 KCl, 10 MgCl_2 , 10 CaCl_2 .

(b) The outward current at +80 and +100 mV was the same within experimental error (Fig. 2) in both 100 mM K and 500 mM K SW. Similarly, the outward current at potentials positive to +60 mV was unaffected by cesium (Fig. 4). If the activation kinetics were altered by these external solutions, these measurements would have differed, as was the case with 10 mM K and 10 mM K 440 mM Tris SW (Fig. 6).

(c) The voltage dependence of our current measurements were the same within experimental error for 20 ms duration prepulses to either -20 or 0 mV.

Therefore, we concluded that K, Cs, and Rb do not alter potassium channel activation. All three ions have been reported to alter deactivation, or tail kinetics (Swenson and Armstrong, 1981; Matteson and Swenson, 1982).

Data Acquisition

Data acquisition was the same as described by French and Shoukimas (1981), except that current was sampled at 50 μ s intervals during the prepulse and at 10 μ s intervals during the test step. Correction for linear leakage and capacitive currents was performed off-line by adding three successive current records obtained in response to test voltages V , $-V/2$, and $-V/2$. A nonlinear leakage current was occasionally observed in these experiments, particularly at potentials positive to about +50 mV. Consequently, we also measured the leakage directly with depolarizing steps from holding to test potential. The records in Figs. 1 and 3 have been corrected for leakage and capacitance currents. The records in Figs. 6 and 7 are uncorrected. The data points in all of the experimental current-voltage relations represent corrected values.

Analysis

Data recovery and some of the analyses were performed with a Digital Equipment Corporation (Marlboro, MA) PDP-11/60 computer. Curve fitting was performed using the MLAB (Knott and Shrager, 1972) program implemented on the DecSystem-10 at the Division of Computer

Research and Technology at the National Institutes of Health, Bethesda, MD.

Junction Potentials

The liquid junction potentials between the internal and external solutions were measured with the experimental electrodes and a salt bridge of 3 M KCl in 3% agar, which was used to connect the solutions. The results of this procedure were ≤ 4 mV for all solutions. Corrections for liquid junction potentials have been made in all of the experimental current-voltage relations given in the Results.

Reversal Potentials

The reversal potential for potassium channels is given by $E_K = kT/q \log_e a_{K_o}/a_{K_i}$, when potassium ions are the sole permeant species, where k is the Boltzmann constant, T is the absolute temperature, q is the unit electronic charge, and a_{K_o} and a_{K_i} are the activities of external and internal ions, respectively. We measured E_K in control solutions by determining the potential for which time-dependent current was minimal during single-step depolarizations from holding potential. These measurements were within a few mV of the theoretical E_K for 50, 100, 300, and 500 mM K SW, as determined with bulk ionic concentrations substituted for the respective activities in the above expression. Therefore, we used bulk concentrations throughout this report in our theoretical calculations whenever ion accumulation was minimal. For example, we used $E_K = -26.5$ mV for experiments with 100 mM K SW as the control solution and $V = -20$ mV as the prepulse potential. We did not use the bulk ion concentrations for the analysis of the experiments in Fig. 2 for which a prepulse potential of 0 mV was used. The effect of ion accumulation or depletion in the periaxonal space is significant in these results, as evidenced by the shift in the reversal potential of the current voltage curve from E_K . Consequently, we allowed the external ion concentration to be a variable in our analysis of these results. The prepulse potential for one of the preparations in Fig. 4 was also 0 mV with 100 mM K SW as the control solution. Accumulation was not a significant factor for these results, as evidenced by the consistency of the reversal potential with E_K .

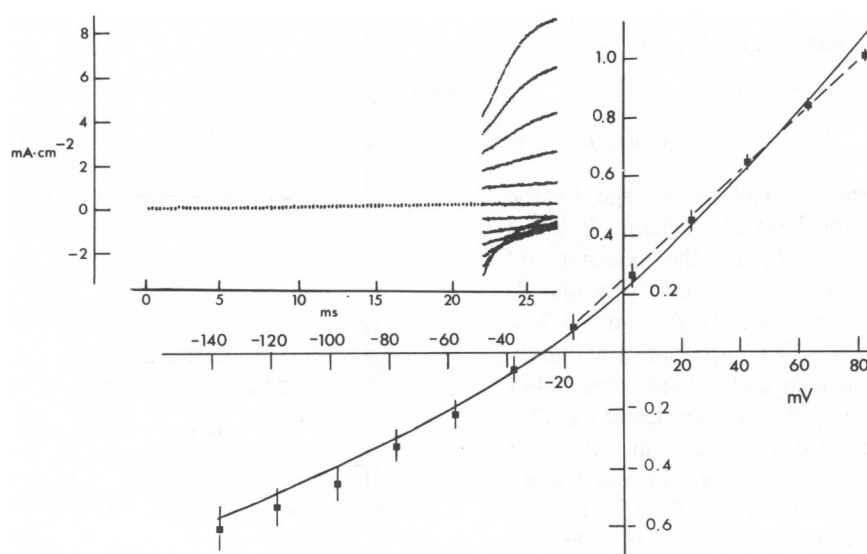


FIGURE 1 Current-voltage relation for 100 mM K SW. The six outward current measurements for each preparation ($n = 10$) were best fit to a straight line, the slope of which was scaled so that the value of the line was 1 at +80 mV. The raw measurements were also appropriately scaled. The data points (■) represent the mean of the scaled measurements and the error bars represent standard deviations from the mean. The solid line is the best fit to the mean results of the GHK equation (Eq. 1). The straight dashed line was drawn by eye through the outward current measurements. Inset: superimposed records, with holding potential = -100 mV; prepulse to -20 mV starting at 2 ms. Axon C8110.

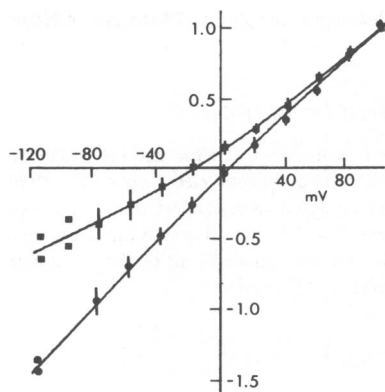


FIGURE 2 Current-voltage relations for axons in 100 mM K (■) and 500 mM K SW (●) ($n = 3$). The results were scaled and pooled as in Fig. 1 with the currents at +100 mV scaled to one. Prepulse potential = 0 mV; holding potential = -80 mV.

RESULTS

Control Current-Voltage Relations

Potassium-channel current of squid axons is, in general, a nonlinear function of driving force, $V - E_r$, where E_r denotes reversal potential, when the external and internal potassium ion concentrations are unequal. This result is illustrated in Fig. 1. The outward currents were very nearly linear (---), but the inward currents displayed a clear curvature or rectification. The data points in Fig. 1 are pooled results from 10 axons. The six outward current measurements for each preparation were fitted to a straight line. The best fit value of the slope was scaled so that the value of the straight-line relation was unity at +80 mV. The solid line (—) is the best fit to these results of the Goldman-Hodgkin-Katz (GHK) equation (Goldman, 1943; Hodgkin and Katz, 1949), which is given by

$$I = P_K F e V / k T [K_o - K_i \exp(eV/kT)] / [1 - \exp(eV/kT)] \quad (1)$$

where I is potassium current, e is electronic charge, k is the Boltzmann constant, F is the Faraday constant, T is the absolute temperature, K_o and K_i are the external and internal potassium ion concentrations, respectively, and P_K is the classically defined permeability coefficient. At $T = 8^\circ\text{C}$, $kT/e = 24$ mV. The GHK equation adequately described the potential dependence of inward current, but it failed to describe accurately the outward currents. This inadequacy is even more apparent when currents from potentials more positive than +80 mV are included, since outward current is approximately a linear function of $V - E_r$ for potentials at least as positive as $V = +200$ mV (French and Wells, 1977).

Results similar to those in Fig. 1 are shown in Fig. 2 for axons bathed in 100 and 500 mM K SW ($n = 3$). The protocol differed slightly in these experiments in that a prepulse to $V = 0$ mV was used, rather than -20 mV, as a

compromise between the different values of E_K with 100 and 500 mM K SW. The outward current was approximately the same for both levels of potassium at potentials positive to about +80 mV. This result is consistent with several other experiments involving various different levels of K_o . The effect of K_o on outward current generally decreased with increasingly positive test potentials. Inward current was significantly more sensitive to K_o , as the results in Fig. 2 illustrate. Accumulation and depletion of ions in the periaxonal space during the prepulse was a factor in these results, as evidenced by the difference between the theoretical E_K and the reversals of the current voltage curves in Fig. 2. Consequently, we let K_o be a variable parameter in fitting Eq. 1 to these results. The best fit values of K_o were 158.8 and 377.2 mM with the bulk concentrations of 100 and 500 mM, respectively. The results of the fitting procedure are illustrated by the solid lines in Fig. 2. The GHK equation provides a better fit for these results than those in Fig. 1, possibly because the difference between K_i and the effective value of K_o is less, and the scatter in the experimental results is somewhat larger.

We assumed in the above analysis that sodium ions do not influence the shape of the current voltage curve, primarily because of the consistency of reversal potential with E_K in experiments that minimized the effects of potassium ion accumulation and depletion (Methods). Apparently, Na ions do not permeate the potassium channel for potentials in the -50 to +20 mV range with $50 \text{ mM} \leq K_o \leq 500 \text{ mM}$. It appears unlikely that they have an influence on the current voltage curve at potentials more

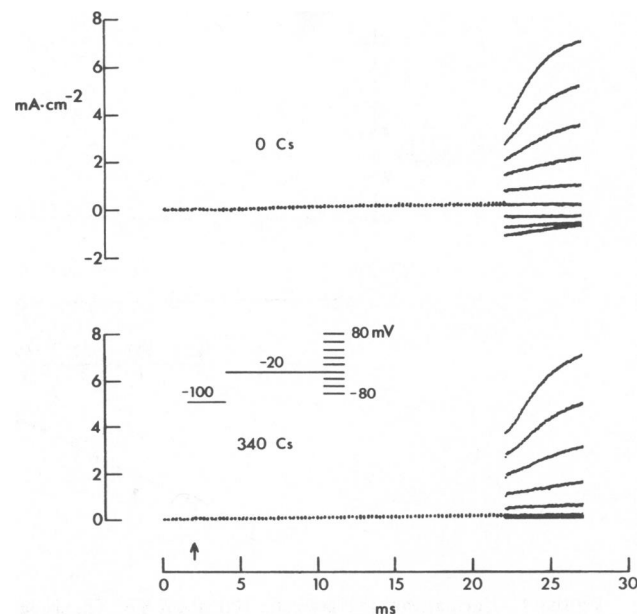


FIGURE 3 Superimposed records for an axon in 100 mM K SW and 100 mM K 340 Cs SW. Holding potential = -100 mV; prepulse to -20 mV starting at 2 ms (arrow). Axon C8112.

positive than +20 mV, since external K ions do not have a significant effect in this potential range. The shape of the current voltage curve for $V \leq -50$ mV suggests that Na ions do not have a significant effect in this range either, since a secondary increase of inward current would be evident if Na ions permeated the channel at $V \leq -50$ mV.

Control experimental results similar to those in Fig. 1 and Fig. 2 appear elsewhere in the literature (French and Wells, 1977; Eaton and Brodwick, 1980; Swenson and Armstrong, 1981). We are merely emphasizing the nonlinearity of the control current voltage curve more than in previous reports.

Effects of External Cs on Outward Current

Our primary interest in the effects of cesium concerned conditions in which the cesium concentration was greater than the potassium concentration. Experimental records from an axon bathed in 100 mM K SW and 100 mM K 340 mM Cs SW are shown in Fig. 3. Inward current was almost completely blocked by the test solution. We also noted a small, but clear reduction of outward current compared to control, particularly for the 0-mV test potential. The degree of block was $40 \pm 6\%$ ($n = 8 \pm \text{SD}$). The block was relieved at more positive potentials. At $V = 40$ mV, it was $17\% \pm 10\%$, and at $V = 80$ mV, the test and control records superposed almost exactly. A small kinetic feature was apparent in the test record immediately following the +80 mV step. More typically, we observed a lack of an effect of cesium containing solutions on activation kinetics (Methods).

Composite current voltage curves for several different cesium concentrations are shown in the left-hand panel of

Fig. 4. The N-shaped voltage dependence of inward current in the test solutions was similar to the results reported by Adelman and French (1978). A reduction of outward current was observed for 100 mM K 200 mM Cs SW and 100 mM K 340 mM Cs SW. We did not observe a clear effect on outward current for solutions containing 100 mM Cs or less.

The potassium channel reversal potential, E_K , appeared to be unaffected by cesium. That is, cesium ions appeared to be unable to pass through the channel in the vicinity of E_K for solutions containing 100 mM K. They apparently were able to permeate the channel at more negative potentials, as indicated by a slight secondary increase in inward current which we observed in some preparations at $V = -120$ and -140 mV. Adelman and French (1978) reported a similar effect.

The effects of high cesium on outward current with low K SW as the control solution are shown in Fig. 5. The degree of blockade compared with control was about the same as the results in Fig. 4.

Effects of Tris on Potassium Currents

We did not observe an augmentation of outward current by cesium in our experiments. We tested the hypothesis of Adelman and French (1978) that their earlier report of such an effect (French and Adelman, 1976 *b*) may have been attributable to Tris ions. We measured currents in 10 mM K SW and 10 mM K 440 mM Tris SW solutions. The records in Fig. 6 represent activation kinetics for these conditions. The data points represent current voltage relations for the same axon during the 10 mM K 440 mM Tris SW condition and following wash back to the 10 mM K SW control solution. The high Tris SW appeared to

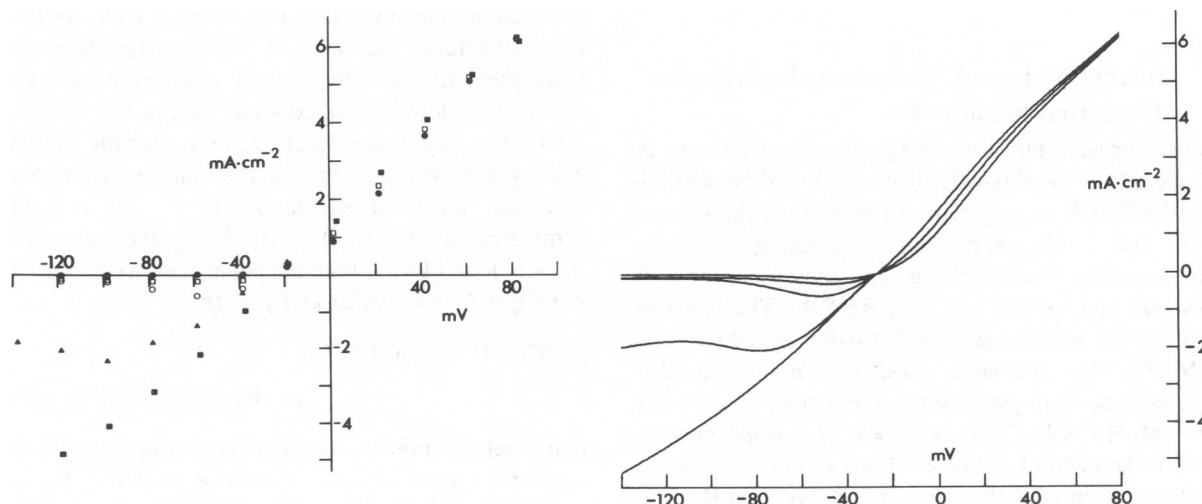


FIGURE 4 Composite current-voltage relations for Cs SW. Left-hand panel: experimental measurements for 0 (■), 100 (○), 200 (□), and 340 mM Cs (●); axon C8130, prepulse = 0 mV; and 5 mM Cs (▲), axon C8152, prepulse = -20 mV. The 5 Cs results were scaled so that the best-fit straight line to the outward currents was the same as that for the 0 Cs results. Right-hand panel: theoretical description for the Cs current-voltage curves as described in the text for 0, 5, 100, 200, and 340 mM Cs. The outward current portion of the 100 mM Cs current-voltage curve has been deleted for the sake of clarity.

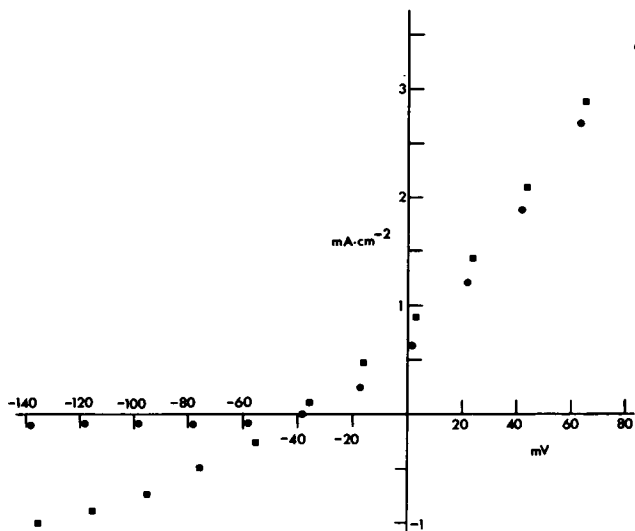


FIGURE 5 Current-voltage relations for 10 mM K SW (■) and 10 mM K 340 Cs SW (●). Axon C8181.

modify channel kinetics. For example, the test record to +80 mV did not result in the same level of peak outward current as the control record. An explanation for this effect is that ion accumulation had a relatively longer time to reduce outward current by changing the effective E_K due to the slower kinetics in 10 mM K 440 mM Tris SW. The current voltage relations in Fig. 6 indicated a lack of voltage-dependent block by Tris. Therefore, we attributed the reduction of current at the end of a 20 ms prepulse to -20 mV in 440 mM Tris SW to a slowing of activation kinetics. A similar effect has been reported for snail neurons by Junge (1982). The effect of Tris appears to be similar to the effects on channel gating of nonelectrolytes, such as sucrose and mannitol, reported by French et al. (1981).

Current-Voltage Relations in the Presence of External Rubidium

Our results for rubidium containing solutions are shown in Figs. 7 and 8 (left-hand panel). The addition of 10 mM Rb to 100 mM K SW clearly reduced current in the inward direction, and it also had a slight blocking effect on outward current. The blockade was increased in both directions by 100 mM K 100 mM Rb SW. The block of outward current was increased still further by 100 mM K 340 mM Rb SW. The latter condition also produced a larger inward current compared to the results in 100 mM K 100 mM Rb SW. That is, block of inward current appeared to be partially relieved. Both E_r and membrane current were essentially the same in 0 K 340 mM Rb SW as compared to 100 mM K 340 mM Rb SW. The current voltage curves for 100 mM K 100 mM Rb SW and 100 mM K 340 mM Rb SW were nearly flat in the vicinity of E_r . This blockage was relieved in both directions by increases in the driving force. The voltage dependence of

inward current was especially suggestive of this effect. The inward current of the control current voltage curve displayed a slight rectification in the direction predicted by the GHK equation, as described above. The 10, 100, and 340 mM Rb results demonstrated different curvatures. The 100 mM K 10 mM Rb SW current voltage curve was nearly a straight line for potentials more negative than ~20 mV below E_r , whereas the 100 mM K 100 mM Rb and 100 mM K 340 mM Rb SW current voltage curves had curvatures in the opposite direction of the control. That is, their slope conductance increased for increasingly negative test potentials. A similar result has been reported for the effects of rubidium on the inward rectifier of frog skeletal muscle (Standen and Stanfield, 1980).

A Model

We have described the theory behind our results using a variation of the original Hodgkin and Keynes (1955) knock-on, single-file diffusion model of ion permeation through a channel containing one or more ion selective sites. Following Hodgkin and Keynes (1955), we assumed that each of the sites was occupied by an ion and that ion motion was initiated only when permeant ions from either side of the membrane struck the ions within the channel with sufficient energy to overcome the forces that tended to keep the ions in the channel in place. We let the average time interval between collisions from the internal and external solutions be \bar{t}_i and \bar{t}_o , respectively. We assumed that these quantities were functions of ion concentration. That is, $\bar{t}_i = \bar{t}_i K_i^{-1}$ and $\bar{t}_o = \bar{t}_o K_o^{-1}$. Not all collisions resulted in movement, particularly if the potential gradient opposed the direction of motion. Consequently, we let $p_+(V)$ be the voltage-dependent probability that the ions in the channel moved outward when a collision from the internal solution occurred. Similarly, we let $p_-(V)$ be the probability that the channel ions moved inward when a collision from the external solution occurred. A collision that displaced ions from their sites in the channel was termed a successful collision. Following Hodgkin and Keynes (1955), we let an ion that caused a successful collision enter the channel and occupy the site adjacent to the solution from which it emerged. We assumed that $p_+(V \rightarrow -\infty) = 0$ and, by symmetry, $p_-(V \rightarrow \infty) = 0$. We further assumed that $p_+(V) + p_-(V) = 1$ at all potentials. Moreover, we let $p_+(V)/p_-(V) = \exp(eV/kT)$, so that

$$p_-(V) = [1 + \exp(eV/kT)]^{-1} \text{ and}$$

$$p_+(V) = \exp(eV/kT)p_-(V). \quad (2)$$

Our final assumption was that the frequency of successful collisions was an increasing function of driving force. That is, we assumed that the collision frequency from either side was proportional to $f(V - E_r)$ with $f(V = E_K) = 1$ and $f(V \neq E_K) > 1$.

The net ionic current of the model was

$$I = Ne\bar{t}^{-1} f(V - E_r)[K_i p_+(V) - K_o p_-(V)] \quad (3)$$

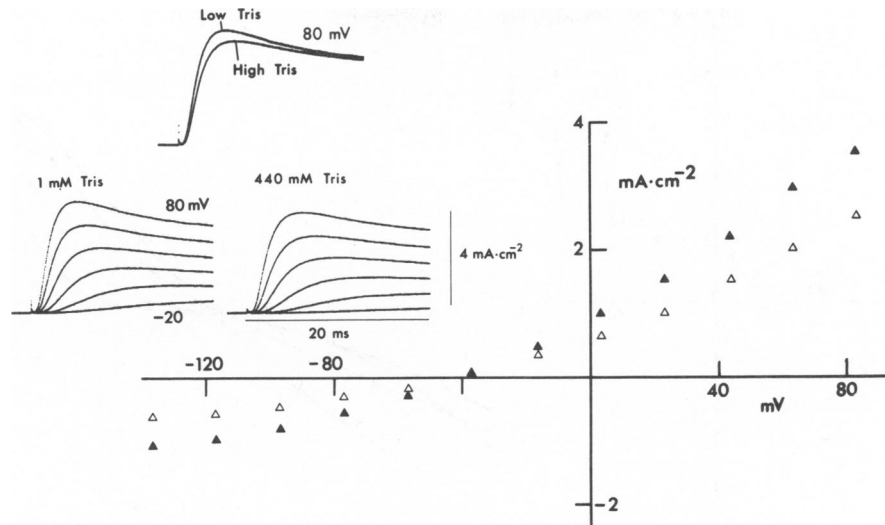


FIGURE 6 Current-voltage relations for 10 mM K SW (▲) and 10 mM K 440 Tris SW (Δ). *Inset*: experimental records for single step depolarizations from holding potential (-100 mV). The two records at +80 mV in the top portion of the inset provide a direct illustration of the change in kinetics produced by the 440 Tris SW. Axon C8180.

where N represents channel density. In control conditions $E_r = E_K$. Empirically, we found that Eq. 3 satisfactorily described our control current voltage curve in 100 mM K SW, provided that $f(V - E_r) = 1 + (V - E_r)/C$ for $V < E_r$ and $f(V - E_r) = 1 + [(V - E_r)/D]^3$ for $V > E_r$, where C and D are constants.

We incorporated the effects of cesium and rubidium into the model by assuming that a Rb or Cs ion entered a channel in knock-on manner similar to that of a K ion. The innermost site of the channel was assigned Rb and Cs specific properties. (From this point forward, we replace Rb or Cs by the symbol X). When an X ion occupied the

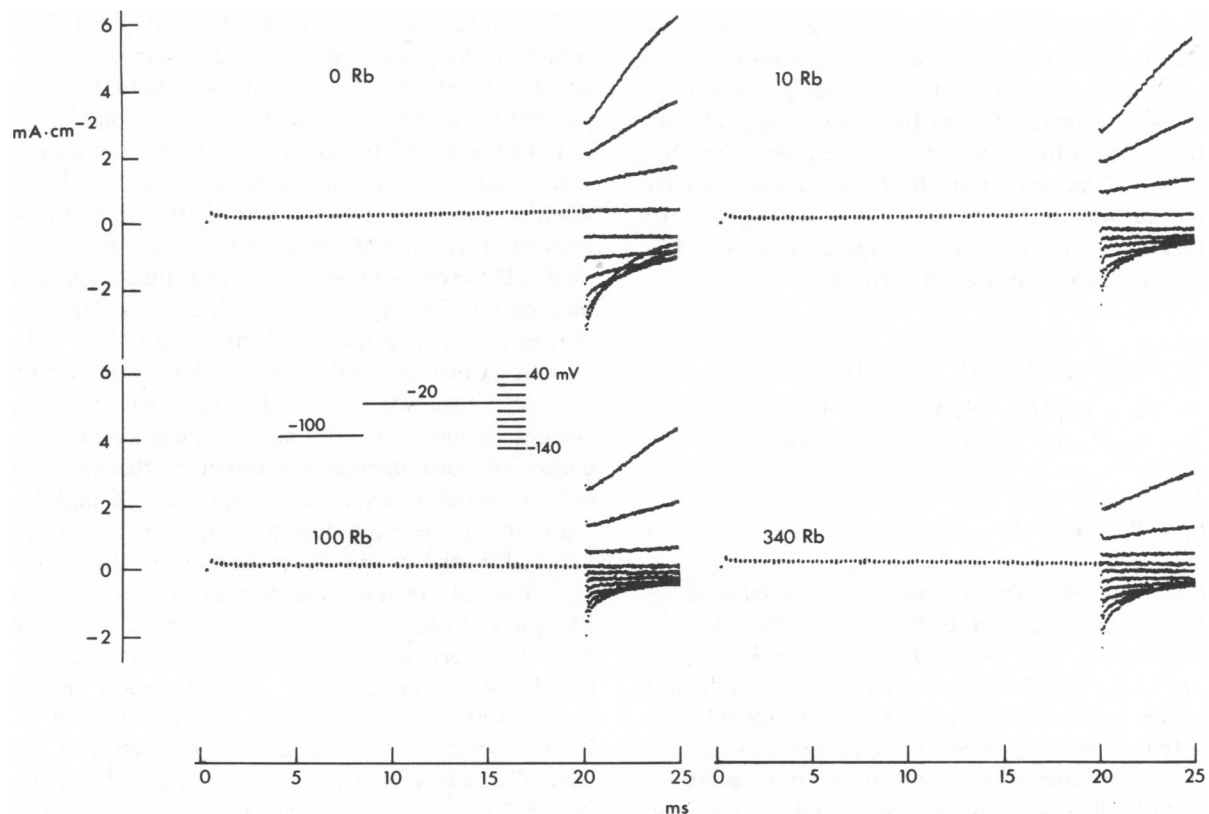


FIGURE 7 Experimental measurements for Rb SW. Axon C8150.

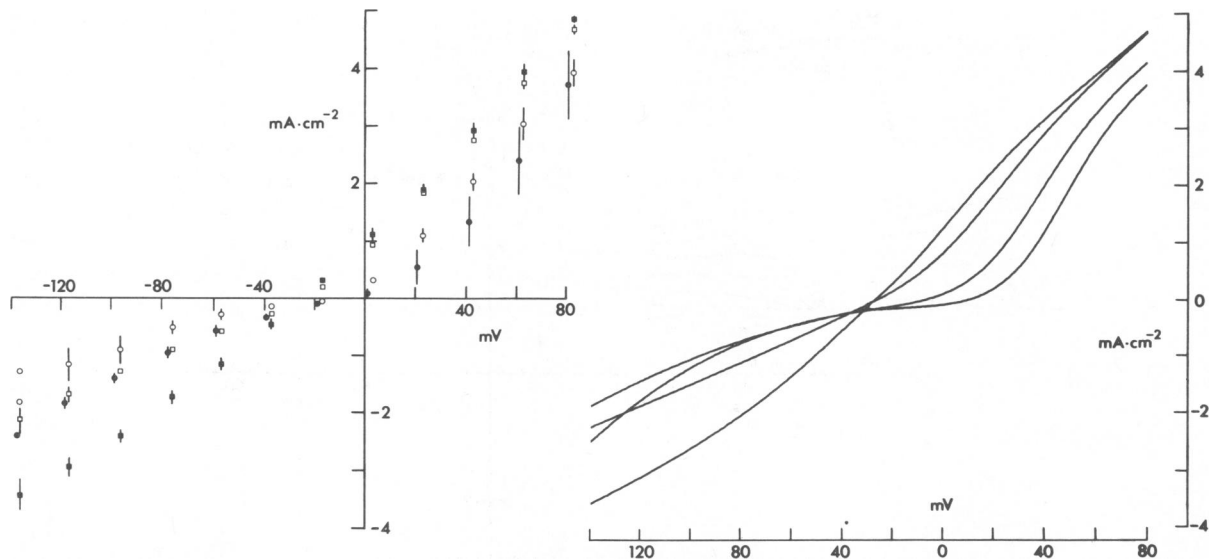


FIGURE 8 Current-voltage relations for Rb SW. Left-hand panel: experimental measurements ($n = 3$) for 0 (■), 10 (□), 100 (○), and 340 mM Rb (●). Prepulse = -20 mV. Right-hand panel: theoretical description of the rubidium current-voltage curves, as described in the text for 0, 10, 100, and 340 mM Rb. The 100 and 340 mM Rb results nearly overlap between -30 and -70 mV. The 340 mM Rb result curves downward, away from the 100 mM Rb result at more negative potentials. It crosses over the 10 mM Rb result at ~ -125 mV.

innermost site, we assumed that it was knocked into the internal solution with probability β ($\beta \leq 1$) by an external collision, which would have been successful in control conditions. Similarly, we let γ be the probability for an X ion to be knocked back from the innermost site to the adjacent outward site in the channel by a collision that would have been successful in control. The effects of the blocking ions were represented by different states of the channel to which we assigned probabilities of occupancy. For a two-site channel, P_{∞} was the probability that both sites were occupied by K ions, P_{ox} was the probability that an X ion was in the outermost site, P_{xo} was the probability that an X ion was in the innermost site, and P_{xx} was the probability that both sites were occupied by X ions. The transitions between states were described by

$$\begin{aligned}\bar{t} \frac{dP_{\infty}}{dt} &= \bar{t} \dot{P}_{\infty} = p'_+ P_{ox} + (1-r)p'_- \beta P_{xo} - r p'_- P_{\infty} \\ \bar{t} \dot{P}_{ox} &= r p'_- P_{\infty} + \gamma p'_+ (P_{xx} + P_{xo}) - (p'_+ + p'_-) P_{ox} \\ \bar{t} \dot{P}_{xo} &= (1-r)p'_- \beta (P_{ox} + P_{xx}) - (p'_+ + \beta p'_-) P_{xo} \\ \bar{t} \dot{P}_{xx} &= r p'_- P_{ox} - (p'_+ + (1-r)\beta p'_-) P_{xx} \\ P_{\infty} + P_{ox} + P_{xo} + P_{xx} &= 1\end{aligned}\quad (4)$$

where r denoted the probability that an X ion entered the channel when a successful collision from the external solution occurred. Moreover, p'_+ denotes $p_+ K_i$ and p'_- denotes $p_+ (K_o + \beta X)$, where βX represents the effective concentration of the test ion that was permeant. We assumed that \bar{t} was on the order of microseconds, or less. Consequently, the quantities of interest were the solutions to Eq. 4 with all time derivatives set equal to zero. The determination of P_{∞} , P_{ox} , P_{xo} , and P_{xx} was a straightfor-

ward, though somewhat tedious algebraic exercise. The net ionic current in the presence of either Cs or Rb was

$$I = Ne\bar{t}^{-1} f(V - E_r) \{p'_+ P_{\infty} - p'_- [P_{ox} + \beta X(P_{xo} + P_{xx})]\}. \quad (5)$$

We implemented the model by fitting Eq. 3 to the control current voltage curves in Figs. 4 and 8. This procedure yielded best fit estimates for both $Ne\bar{t}^{-1}$ and the parameters B and C in the above expressions for $f(V - E_r)$. The appropriate values for the ion concentrations in Eqs. 3 and 5 were used throughout the analysis. The remaining free parameters in Eq. 5 were β , γ , and r . The number of sites in the channel was also a parameter of the model. However, we found that a two-site channel gave the best description of all our results, particularly the N -shaped voltage dependence of the cesium block of inward current. A one-site model gave an N -shaped current voltage curve that was too broad; a three-site model gave a current voltage curve that had too steep a voltage dependence. The most important parameter, other than number of sites for the cesium data, was r , since we found that $\gamma = 1$ and $\beta \approx 0$ were appropriate. That is, a cesium ion was knocked back toward the outward direction from the innermost site in the same manner as a K ion ($\gamma = 1$). Moreover, it had a very small probability of being knocked from the innermost site to the internal solution ($\beta \approx 0$). The specific best fit values of r and β for the theoretical curves in Fig. 4 are given in Table II. The results in Fig. 4 for inward current correspond to Cs = 0, 5, 100, 200, and 340 mM. The results for outward current correspond to Cs = 0, 200, 340 mM. The model provided an adequate fit to our experimental data.

TABLE II
BEST FIT MODEL PARAMETERS

Concentration	r	Cesium			α'	
		β	α	α'		
(mM)						
5	0.0063	0.0018	0.12	1.73		
50*	0.125	0.0018	0.29	1.08		
100	0.42	0.01	0.725	1.86		
200	0.72	0.007	1.3	2.83		
340	0.99	0.0006	—	—		

Concentration	β_0	β_1	Rubidium		α	γ
			$E^*(\text{mV})$	r		
(mM)						
10	0	0.4	-150	0.184	2.2	0.008
100	0.03	1.1	-130	0.73	2.7	0.008
340	0.03	1.1	-130	0.99	—	0.004

*Results with 50 mM Cs are not shown in Fig. 4.

The simplest interpretation of the concentration dependence of the parameter r was

$$r = \alpha \text{Cs} / (\alpha \text{Cs} + K_0) \quad (6)$$

where α was the relative affinity of a Cs ion for a K channel compared with a K ion. We were surprised to find that the results for α (Table II) depended upon cesium concentration. Our analysis of the Adelman and French (1978) data gave a similar result. By contrast, our analysis of cesium block of the inward rectifier in frog skeletal muscle (Gay and Stanfield, 1977) and in starfish echinoderm (Hagiwara et al., 1976) gave a value of α that was independent of external cesium (J. R. Clay and M. F. Shlesinger, unpublished). That is, cesium appears to compete for entry into the squid axon potassium channel in a different manner from other preparations, at least within the framework of our analysis. An alternative assumption for the concentration dependence of r is

$$r = [\alpha' \text{Cs} / (\alpha' \text{Cs} + K_0)]^2 \quad (7)$$

One interpretation of Eq. 7 is that two Cs ions are required in the vicinity of a channel for either one to produce a successful knock-on collision. The corresponding results for α' given in Table II are roughly independent of Cs, which suggests that Eq. 7 may be an appropriate expression for r for external solutions containing cesium.

The blockade of outward current by cesium was a natural outcome of the model. That is, we found that the best-fit parameters for block of inward current automatically gave the appropriate degree of block of outward current.

Our analysis of the Rb results in Fig. 7 required a modification of our assumptions concerning γ and β . We found that Eqs. 4 and 5 with $\gamma = 1$ predicted an insufficient block of outward current. The theoretical results in Fig. 4 describe the maximum degree of blockade of outward

current which is inherent in the knock-on process without further assumptions. We found that a relatively small value of γ was required to enhance this effect. That is, an Rb ion was not easily knocked back in the outward direction once it reached the innermost site of the channel. A further modification of the model concerned the parameter β . We found it necessary to assign a relatively significant value to this parameter so that the channel was permeable to rubidium at all potentials. Moreover, the data in Fig. 8 required a voltage dependence for β . We found that an appropriate expression for this feature of the model was

$$\beta = \beta_0 + \beta_1 / \{1 + \exp[(V - E^*)/50]\} \quad (8)$$

where β_0 , β_1 , and E^* are constants. The best-fit values for these parameters, as well as for r and γ for the data in Fig. 8, are given in Table II. The results for α for 10 and 100 mM Rb suggest that Rb may compete with K on a one-to-one basis for K channels, in contrast to Cs. The other parameters are also at least roughly independent of Rb concentration. The model gave an adequate description of our results. Moreover, the theoretical current voltage curve with parameters appropriate to 100 mM K 340 mM Rb SW was changed very little when K_0 was set equal to zero. That is, the model also successfully described the lack of an effect of 100 mM K_0 on E_r and on membrane currents in the presence of 340 mM Rb.

DISCUSSION

Our results indicate a significant reduction of outward potassium ion flux in squid axons by external cesium and rubidium ions. This result is somewhat unusual, since the primary emphasis in the literature on the effects of these ions on potassium channels has been on currents in the direction away from the side of the membrane on which they are placed. These results have led to a theoretical picture in which a blocking ion gets swept into a channel by other ions and by membrane potential. The voltage dependence of the effects of a blocking ion arises from the fact that it must move through some fraction of the membrane field before reaching its blocking site within the channel. Our results are consistent with this scheme. Both permeant and blocking ions have a small but finite probability of entering a channel against an opposing driving force because of their thermodynamic motion. However, relatively large concentrations of blockers are required to reveal these back flux effects.

Tracer flux measurements in the presence of cesium or rubidium have apparently not been carried out on squid axons. A reduction of tracer efflux has been reported for the inward rectifier of frog skeletal muscle by external Rb with $K_0 > 45$ mM (Spalding et al., 1981, 1982). Also, the results of Standen and Stanfield (1980) illustrate a significant block of net outward current of the inward rectifier by Rb for potentials > 50 mV positive to E_r . The reduction of

block that we are reporting for potentials 50 to 100 mV positive to E_r may be difficult to observed for the inward rectifier, because the rectification in control preparations reduces current to near zero for $V > E_r + 50$ mV.

Our theoretical analysis illustrates that a model of single-file diffusion with a knock-on character can successfully describe voltage-dependent blockade of potassium channels by small ions. In recent years a different view of single file diffusion has evolved based on chemical reaction rate theory (Glasstone et al., 1941; Eyring et al., 1949; Hille and Schwartz, 1978). In this model, ions are viewed as hopping in single file along a linear sequence of energy barriers and binding sites, with rate constants that depend upon barrier heights, membrane potential, and interionic repulsion. The primary difference between knock-on and the Eyring rate-theory approach is the manner in which motion of ions in the channel occurs. The knock-on model requires an external ion to strike the channel before ions can move (Hodgkin and Keynes, 1955). Moreover, all sites in the channel must be occupied by ions. In contrast, all sites are usually not occupied in Eyring rate theory. In fact, an ion can move from one site to an adjacent site only when the adjacent site is vacant (Hille and Schwartz, 1978). The hypothesis that all sites are occupied appears to be incorrect, in general, based on the observations of Begenisich and DeWeer (1980), who found that the potassium flux ratio exponent in squid axons bathed in 20 or 40 mM K_o depended on membrane potential. The flux ratio exponent of the knock-on model is independent of V . However, the assumption of fully occupied sites is, at least, more reasonable for $K_o = 100$ mM than for $K_o = 20$ or 40 mM. Moreover, the high ion activity regime allows a significant simplification for the ion flux predicted by Eyring rate theory, which permits a convenient comparison of this approach with knock-on theory. Hille and Schwartz (1978) have shown that, in this regime, Eyring rate theory predicts a current for a symmetrical two-site channel, which is given by

$$I \sim K_o^{-1} \exp(eV/2kT) - K_i^{-1} \exp(-eV/2kT). \quad (9)$$

The relevant expression for knock-on theory [Eqs. 2 and 3 with $f(V - E_r) = 1$] is

$$I \sim [\exp(eV/2kT) + \exp(-eV/2kT)]^{-1} [K_o^{-1} \exp(eV/2kT) - K_i^{-1} \exp(-eV/2kT)]. \quad (10)$$

In the limit $V \rightarrow +\infty$, Eq. 9 predicts $I \rightarrow K_o^{-1} \exp(eV/2kT)$, whereas Eq. 10 predicts $I \rightarrow 1/K_o$. That is, Eq. 9 diverges because the rate-limiting step for ion motion is the height of the energy barriers, which vanishes in the limit of large potentials. Eq. 10 is a saturating function of V , because the limiting step in the knock-on model is the frequency of successful collisions. We have circumvented the latter effect by hypothesizing that the rate of successful collisions depends upon $V - E_r$, which seems physically reasonable to us, although the specific form we chose for

$f(V - E_r)$ is admittedly ad hoc. In any case, a linear current voltage curve, which the data of French and Wells (1977) suggest for outward currents up to at least $V = +200$ mV, is a severe constraint for any single-file diffusion model.

A more serious shortcoming of the knock-on approach is its failure to predict saturation of ionic current as the ion concentrations are raised. This effect has been reported for sodium channels in nerve (Begenisich and Cahalan, 1979), and it appears to be valid for potassium channels, as well, based on the measurements of Coronado et al. (1980) from K channels reconstituted in lipid bilayers from a sarcoplasmic reticulum vesicles preparation. Our measurements in Fig. 2 appear to be below the range of K_o for which saturation occurs, since the slope conductance of inward current in 500 mM K SW, with an effective K_o of 377 mM, was about two times greater than that of 100 mM K SW with an effective K_o of 158 mM (Results). The difference in these effective K_o values is approximately consistent with the change in inward current, as predicted by knock-on theory. Further experiments may reveal a saturation effect in squid potassium channels, which would be difficult to reconcile with our model. To describe this effect the collision factor $1/\bar{t}$ would have to be a saturating function of ion activity. Such a mechanism cannot be ruled out a priori, although we are unable to devise a reasonable theoretical scheme which incorporates this effect.

The primary strength of the knock-on model is that it provides a reasonably compact description of complex voltage-dependent conductance in the presence of a permeant ion and a second ionic species which acts at least partly as a blocker. Moreover, it reveals the relationship between degree of block and concentration of the blocking ion. As we have shown, these results provide insight to the number of sites in the channel, the nature of the competition between the blocker and the permeant species, and the relative effects of different blockers.

Received for publication 14 April 1982 and in final form 15 November 1982.

REFERENCES

- Adelman, W. J. Jr. 1971. Electrical studies of internally perfused squid axons. In *Biophysics and Physiology of Excitable Membranes*. W. J. Adelman, Jr., editor. Van Nostrand Reinhold Co. NY. 274-319.
- Adelman, W. J. Jr., and R. J. French. 1978. Blocking of the squid axon potassium channel by external cesium ions. *J. Physiol. (Lond.)* 276:13-25.
- Adelman, W. J. Jr., and J. P. Senft. 1966. Voltage clamp studies of the effects of internal cesium ions on sodium and potassium currents in the squid giant axon. *J. Gen. Physiol.* 50:279-293.
- Begenisich, T., and M. Cahalan. 1979. Non independence and selectivity in sodium channels. In *Membrane Transport Processes*. C. F. Stevens and R. W. Tsien, editors. Raven Press, New York. 3:113-122.
- Begenisich, T., and P. De Weer. 1980. Potassium flux ratio in voltage-clamped squid giant axons. *J. Gen. Physiol.* 76:83-98.
- Bezanilla, F., and C. M. Armstrong. 1972. Negative conductance caused by entry of sodium and cesium ions into the potassium channels of squid axons. *J. Gen. Physiol.* 60:588-608.

- Chandler, W. K., and H. Meves. 1965. Voltage clamp experiments on internally perfused giant axons. *J. Physiol. (Lond.)*. 180:788–820.
- Clay, J. R., and M. F. Shlesinger. 1977. Random walk analysis of potassium fluxes associated with nerve impulses. *Proc. Natl. Acad. Sci. USA*. 74:5543–5546.
- Clay, J. R., and M. F. Shlesinger. 1982. Effects of external Cs and Rb on outward K currents in squid axons. *Biophys. J.* 37(2, Pt. 2):16 a. (Abstr.)
- Coronado, R., R. L. Rosenberg, and C. Miller. 1980. Ionic selectivity, saturation, and block in a K⁺-selective channel from sarcoplasmic reticulum. *J. Gen. Physiol.* 76:425–446.
- Eaton, D. C., and M. S. Brodwick. 1980. Effects of barium on the potassium conductance of squid axon. *J. Gen. Physiol.* 75:727–750.
- Eyring, H., R. Lumry, and J. W. Woodbury. 1949. Some applications of modern rate theory to physiological systems. *Rec. Chem. Prog.* 10:100–114.
- Fishman, H. 1973. Low impedance capillary electrode for wide band recording of membrane potential in large axons. *IEEE Trans. Biomed. Eng.* BME-20:380–382.
- French, R. J., and W. J. Adelman, Jr. 1976 a. Competition, saturation, and inhibition—ionic interactions shown by membrane ionic currents in nerve, muscle, and bilayer systems. *Curr. Top. Membr. Transp.* 8:161–207.
- French, R. J., and W. J. Adelman, Jr. 1976 b. A capricious “blocking” ion. Cesium can increase potassium channel currents. *Biophys. J.* 16(2, Pt. 2):189 a. (Abstr.)
- French, R. J., and J. J. Shoukimas. 1981. Blockage of squid axon potassium conductance by internal tetra-*N*-alkylammonium ions of various sizes. *Biophys. J.* 34:271–291.
- French, R. J., J. J. Shoukimas, M. S. Brodwick, and D. C. Eaton. 1981. Solution microviscosity modulates the kinetics of K-channel block by tetraethanolammonium. *Biophys. J.* 33(2, Pt. 2):71 a. (Abstr.)
- French, R. J., J. J. Shoukimas, and R. Mueller. 1979. Voltage dependence of K-channel block by small cations. *Biophys. J.* 25(2, Pt. 2):307 a. (Abstr.)
- French, R. J., and J. B. Wells. 1977. Sodium ions as blocking agents and charge carriers in the potassium channel of the squid giant axon. *J. Gen. Physiol.* 70:707–724.
- Gay, L. A., and P. R. Stanfield. 1977. Cs⁺ causes a voltage-dependent block of inward K currents in resting skeletal muscle fibres. *Nature (Lond.)*. 267:169–170.
- Glasstone, S., K. J. Laidler, and H. Eyring. 1941. *The Theory of Rate Processes*. McGraw Hill, Inc. New York. 1–611.
- Goldman, D. E. 1943. Potential, impedance, and rectification in membranes. *J. Gen. Physiol.* 27:37–60.
- Hagiwara, S., S. Miyazaki, and N. P. Rosenthal. 1976. Potassium current and the effect of cesium on this current during anomalous rectification of the egg cell membrane of a starfish. *J. Gen. Physiol.* 67:621–638.
- Heckman, K. 1963. In *Funktionell und Morphologische Organization der Zelle*. P. Karlson, editor. Springer-Verlag, Berlin. 241.
- Hille, B. 1973. Potassium channels in myelinated nerve. Selective permeability to small cations. *J. Gen. Physiol.* 61:669–686.
- Hille, B., and W. Schwarz. 1978. Potassium channels as multi-ion single-file pores. *J. Gen. Physiol.* 72:409–442.
- Hladky, S. B. 1965. The single file model for the diffusion of ions through a membrane. *Bull. Math. Biophys.* 27:79–86.
- Hladky, S. B., and J. D. Harris. 1967. An ion displacement model. *Biophys. J.* 7:535–543.
- Hodgkin, A. L., and B. Katz. 1949. The effect of sodium ions on the electrical activity of the giant axon of the squid. *J. Physiol. (Lond.)*. 108:37–77.
- Hodgkin, A. L., and R. D. Keynes. 1955. The potassium permeability of a giant nerve fiber. *J. Physiol. (Lond.)*. 128:61–88.
- Junge, D. 1982. Reduction of outward currents in snail neurons by replacement of external potassium. *Biophys. J.* 37(2, Pt. 2):183 a. (Abstr.)
- Knott, G. D., and R. I. Shrager. 1972. On-line modeling by curve fitting. *Proceedings of SIGGRAPH Computers in Medicine Symposium ACM, SIGGRAPH Notices*. 6:138–151.
- Matteson, D. R., and R. P. Swenson, Jr. 1982. Permeant cations alter closing rates of K channels. *Biophys. J.* 37(2, Pt. 2):17 a. (Abstr.)
- Pickard, W. F., J. Y. Lettvin, J. W. Moore, M. Takata, J. Pooler, and T. Bernstein. 1964. Cesium ions do not pass through the membrane of the giant axon. *Proc. Natl. Acad. Sci. USA*. 52:1177–1183.
- Standen, N. B., and P. R. Stanfield. 1980. Rubidium block and rubidium permeability of the inward rectifier of frog skeletal muscle fibers. *J. Physiol. (Lond.)*. 304:415–435.
- Spalding, B., J. Swift, O. Senyk, and P. Horowicz. 1981. Effects of external rubidium on potassium efflux in depolarized frog skeletal muscle. *Biophys. J.* 33(2, Pt. 2):119 a. (Abstr.)
- Spalding, B. C., J. G. Swift, O. Senyk, and P. Horowicz. 1982. The dual effect of rubidium ions of potassium efflux in depolarized frog skeletal muscle. *J. Membr. Biol.* 69:145–157.
- Swenson, R. P. Jr., and C. M. Armstrong. 1981. K⁺ channels close more slowly in the presence of external K⁺ and Rb⁺. *Nature (Lond.)*. 291:427–429.